

Ionic Layering and Overcharging in Electrical Double Layers in a Poisson-Boltzmann Model

Ankur Gupta^{1,2,*}, Ananth Govind Rajan^{1,3}, Emily A. Carter^{1,4,5} and Howard A. Stone^{1,†}


¹*Department of Mechanical and Aerospace Engineering, Princeton University, Princeton, New Jersey 08544, USA*

²*Department of Chemical and Biological Engineering, University of Colorado, Boulder, Colorado 80309, USA*

³*Department of Chemical Engineering, Indian Institute of Science, Bengaluru, Karnataka 560012, India*

⁴*Department of Chemical and Biomolecular Engineering, University of California, Los Angeles, Los Angeles, California 90095, USA*

⁵*Office of the Chancellor, University of California, Los Angeles, Los Angeles, California 90095, USA*

 (Received 2 June 2020; revised 6 September 2020; accepted 30 September 2020; published 30 October 2020)

Electrical double layers (EDLs) play a significant role in a broad range of physical phenomena related to colloidal stability, diffuse-charge dynamics, electrokinetics, and energy storage applications. Recently, it has been suggested that for large ion sizes or multivalent electrolytes, ions can arrange in a layered structure inside the EDLs. However, the widely used Poisson–Boltzmann models for EDLs are unable to capture the details of ion concentration oscillations and the effect of electrolyte valence on such oscillations. Here, by treating a pair of ions as hard spheres below the distance of closest approach and as point charges otherwise, we are able to predict ionic layering without any additional parameters or boundary conditions while still being compatible with the Poisson–Boltzmann framework. Depending on the combination of ion valence, size, and concentration, our model reveals a structured EDL with spatially oscillating ion concentrations. We report the dependence of critical ion concentration, i.e., the ion concentration above which the oscillations are observed, on the counter-ion valence and the ion size. More importantly, our model displays quantitative agreement with the results of computationally intensive models of the EDL. Finally, we analyze the nonequilibrium problem of EDL charging and demonstrate that ionic layering increases the total charge storage capacity and the charging timescale.

DOI: [10.1103/PhysRevLett.125.188004](https://doi.org/10.1103/PhysRevLett.125.188004)

When an electrolyte is in the vicinity of a charged surface, oppositely charged ions from solution migrate toward the surface and form a region of diffuse charge. The combined region of the diffuse charge and the Stern layer, known as the electrical double layer (EDL), is important for applications such as energy storage and conversion [1–4], desalination [5,6], manipulation of colloidal particles [7–10], and soil remediation [11,12], among others. Fundamentally, the EDL impacts diverse physical phenomena, e.g., colloidal stability [13,14], electrokinetic transport in nanochannels [15,16], the structure of ionic liquids [17–20], and the stability of a living cell [21].

The classical perspective on the EDL suggests that the EDL thickness decreases monotonically with an increase in the ion concentration. However, recent reports, both experimental and theoretical, have demonstrated that in the concentrated limit the screening length can increase [18,20,21] with an increase in ion concentration due to a layered arrangement of ions [17,19], which is often characterized through oscillations in ion concentrations.

Typically, the EDL phenomena are modeled through Poisson–Boltzmann (PB) equations due to their analytical simplicity and ease of application to out-of-equilibrium processes. The recent literature on PB models has focused on the effect of finite ion size [22–26], dielectric decrement

[26–30], electrolyte valence [26], and the effect of short-range interactions between ions [26,31–33]. While the inclusion of short-range interactions in PB models, i.e., the fourth-order PB model, commonly known as the Bazant–Storey–Kornyshev (BSK) model, can predict the sign reversal in the electrical potential [31,32,34], it is unable to capture the details of oscillations in ion concentrations and the effect of electrolyte valence on such oscillations.

In contrast, approaches such as classical density functional theory (cDFT) [35–42], integral-equation theories (IET) [43,44], Monte Carlo (MC) simulations [45–49], and molecular dynamics [50–54] are able to predict the oscillations in ion concentrations within the EDL. Therefore, a natural question arises: can ion concentration oscillations be incorporated in a PB model?

To address this knowledge gap, it is crucial to recognize that the continuum approaches such as IET [43,44] and cDFT models [35–42] use the Waisman and Lebowitz result [55,56], which superimposes the hard-sphere and Coulombic potentials and yields a direct correlation function between ions. Therefore, these approaches include the effect of ion size on net electrostatic interactions, a feature typically overlooked in the PB models [22–26,57].

However, the Waisman and Lebowitz result is not compatible with the PB framework. Accordingly, we present an approach to include the effect of ion size on net electrostatic interactions in a PB model. Our model is able to capture the effect of electrolyte valence, concentration, and ion size on the structure of the EDL, including the onset of the layering phenomenon, without any fitting parameters. Most significantly, we demonstrate that the proposed model is in quantitative agreement with computationally intensive models. We also apply our model to the out-of-equilibrium phenomenon of EDL charging and discuss the implications of ionic layering on the charge storage capacity and the charging timescale.

We focus on the scenario where an EDL is in equilibrium with a charged surface. For simplicity, we consider a primitive-electrolyte model and assume that the ions possess a finite size such that the cations and anions are of equal diameter. To include the effect of ion size on net electrostatic interactions in a PB model, we treat a pair of ions as hard spheres when the distance between their centers is less than the diameter of the ions and as point charges otherwise. Since an ion is treated as a hard sphere below the distance of closest approach, the electric potential contributions by the ion are only integrated from the region outside the ion (for a detailed derivation, the reader is referred to Ref. [57]). Together, these effects modify the PB equations as [57]

$$-e\nabla^2\psi(\mathbf{r}) = \sum_i z_i e c_i(\mathbf{r}), \quad (1a)$$

$$c_i[\psi(\mathbf{r})] = \frac{c_{i0} \exp\left\{-\frac{z_i e[\psi(\mathbf{r}) - \psi_s(\mathbf{r})]}{k_B T}\right\}}{1 + \sum_i a^3 c_{i0} (\exp\left\{-\frac{z_i e[\psi(\mathbf{r}) - \psi_s(\mathbf{r})]}{k_B T}\right\} - 1)}, \quad (1b)$$

$$\psi_s[\psi(\mathbf{r})] = -\frac{1}{4\pi} \int_{a/2 < |\mathbf{r} - \mathbf{r}'| \leq a} \frac{\nabla^2 \psi(\mathbf{r}')}{|\mathbf{r} - \mathbf{r}'|} d\mathbf{r}', \quad (1c)$$

where a is the ion diameter, z_i and c_i are the signed valence and concentration of the i th ion type ($i = "+"$ for cation, $i = "-"$ for anion, $z_i > 0$ for cation, and $z_i < 0$ for anion), c_{i0} is the concentration of the i th ion type in the bulk, $\psi(\mathbf{r})$ is the electrical potential, $\psi_s(\mathbf{r})$ is the screened nearest-neighbor potential, ϵ is the electrical permittivity of the solvent, k_B is the Boltzmann constant, T is the temperature, and e is the charge on an electron. We note that ψ_s is essentially a measure of the excluded-volume correction to the electrostatic contributions to the free energy. Equation (1a)–(1c) represent three equations for three unknowns.

When the ions are treated as volumeless, i.e., $a \rightarrow 0$, the original PB equations are recovered. If $\psi_s \rightarrow 0$, the steric PB equations with entropic corrections due to finite ion size are obtained [22,24–26,57]. We highlight that the system of Eq. (1a)–(1c) does not require any additional parameter or an extra boundary condition to describe the details of the EDL.

Furthermore, since c_i is an explicit function of $\psi - \psi_s$, Eq. (1) can be reduced to an integro-differential equation for ψ . We note that such a nonlocal screening potential has not been previously included in PB models of the EDL.

Next, we focus on a one-dimensional scenario where a planar surface with surface charge density σ is in equilibrium with a binary electrolyte (valence z_+ and z_-) such that the concentration of electrolyte far away from the surface (i.e., bulk) is c_b . We denote the direction perpendicular to the surface as x and assume that the charged surface is located at $x = 0$. We denote $\lambda_B = e^2/(4\pi\epsilon k_B T)$ as the Bjerrum length. We define the dimensionless position $X = x/a$, dimensionless potential $\Psi = e\psi/(k_B T)$, and ion volume fraction $\chi_{\pm} = a^3 c_{\pm}$. We impose a constant surface charge boundary condition at $X = 0$ and a Debye–Hückel solution for $X \rightarrow \infty$. We also assume that the ion concentration is zero for $X \leq \frac{1}{2}$, akin to a Stern layer with thickness equal to the ion radius. In addition to the ion valences (z_+ and z_-), the three dimensionless parameters that govern the response are a/λ_B , the dimensionless surface charge density $S = \sigma\lambda_B^2/e$, and the total ion volume fraction in the bulk $\chi_b = (|z_+ + |z_-|)a^3 c_b$ [57].

Our model predicts that the ion concentrations within the EDL can exhibit oscillations, which is a signature of molecular structure. Furthermore, we find that the oscillations are strongly dependent on the valence of the electrolyte. For a positively charged surface, we calculate χ_{\pm} for a 1:1 electrolyte ($z_+ = 1$ and $z_- = -1$) and a 1:3 ($z_+ = 1$ and $z_- = -3$) electrolyte (see Fig. 1). For the 1:1

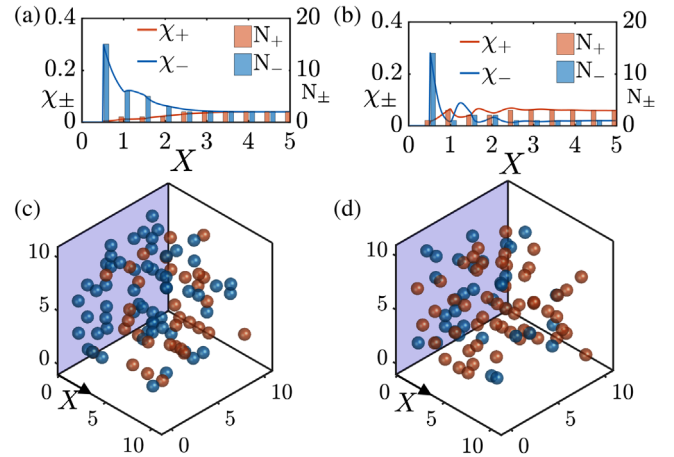


FIG. 1. Prediction of the EDL structure by the proposed model for a charged surface located at $X = 0$. Plot of ion volume fractions (χ_{\pm}) versus the dimensionless distance from the surface (X) for (a) 1:1 electrolyte and (b) 1:3 electrolyte. χ_{\pm} data is converted to the number of ions N_{\pm} in each spatial bin. The N_{\pm} data is transformed into a three-dimensional representation of the EDL structure for (c) 1:1 electrolyte and (d) 1:3 electrolyte. $a = 0.6$ nm, $(|z_+ + |z_-|)c_b = 600$ mM, $T = 298$ K, $\epsilon = 6.94 \times 10^{-10}$ F/m, and $\sigma = 8.7 \times 10^{-2}$ C/m². Anions are shown in blue and cations are shown in red. The distribution of ions in the y and z directions in panels (c) and (d) is random.

electrolyte, χ_{\pm} is monotonic for all X . However, for the 1:3 electrolyte, the oscillations in χ_{\pm} are significant. In fact, even for a positively charged surface, the cation concentration is higher than the anion concentration around $X \approx 1$. Finally, since oscillations in the ion concentrations exist on the order of the ion size and the local maxima in χ_+ coincides with the local minima in χ_- , the EDL has a layered structure of ions.

For a visual representation of the ion concentration distribution, we transformed the χ_{\pm} data to absolute number of ions N_{\pm} in a $10 \times 10 \times 10$ box (Fig. 1, see [57]). We find that for the 1:1 electrolyte, $N_+ < N_-$ for all X . In contrast, for the 1:3 electrolyte, $N_+ > N_-$ for $X = 1$ and displays oscillations in subsequent layers. We emphasize that the structure of the EDL emerges only due to the inclusion of ψ_s in our model [Eq. (1)].

The structure of an equilibrium EDL has implications for out-of-equilibrium electrokinetic phenomena. For instance, in electrophoresis [58], diffusiophoresis [59–61], or charging of the EDL [62,63], the local equilibrium relations of the EDL are used for understanding the physics of the system. To this end, we focus on the phenomenon of overcharging where the colloidal particles display electrophoresis opposite to the expected direction [51–53]. For example, Kubíčková *et al.* [53] showed experimentally that overcharging occurs for trivalent electrolytes, whereas monovalent and divalent electrolytes do not display overcharging. A molecular dynamics model revealed that the net cumulative charge from the surface reverses sign for trivalent electrolytes and thus the colloidal particles behave as oppositely charged particles [53]. However, the existing PB approaches are unable to predict overcharging and the effect of electrolyte valence on it [53].

To explain the phenomenon of overcharging, we evaluate $\Psi(X)$ for the one-dimensional scenario described above. For a positively charged surface, the anion valence significantly influences $\Psi(X)$ [see Fig. 2(a)]. For a 1:1 electrolyte, $\Psi(X)$ decays monotonically. For both 1:2 and 1:3 electrolytes, $\Psi(X)$ reverses sign and has a local minimum, where the minimum is deeper for the 1:3 electrolyte. We plot the dimensionless charge density $P_e = \sum z_i c_i / c_b$ for the three electrolytes in Fig. 2(b). P_e is monotonic for the 1:1 electrolyte, whereas the 1:2 and 1:3 electrolytes show oscillations in P_e . Furthermore, the sign of P_e reverses for 1:2 and 1:3 electrolytes with a stronger reversal for the 1:3 electrolyte. The charge reversal occurs because the cations migrate closer to the wall for multivalent electrolytes [Fig. 1(b)]. The reversal in the sign of $\Psi(X)$ and P_e indicates a tendency of the multivalent electrolytes to cause overcharging.

Next, we investigate the conditions for reversal in the sign of $\Psi(X)$. To this end, we calculate the critical total ion concentration in the bulk above which $\Psi(X)$ reverses the sign, i.e., $\chi_b > \chi_{b,\text{crit}}$ [see Fig. 2(c)]. We plot $\chi_{b,\text{crit}}$ versus a/λ_B for a constant S . For equal a/λ_B , the 1:3 electrolyte

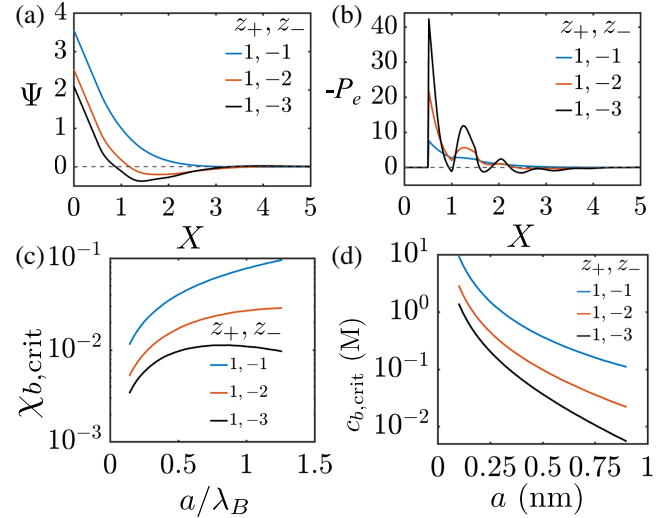


FIG. 2. Effect of electrolyte valence on overcharging. Plot of (a) dimensionless electric potential Ψ and (b) dimensionless charge density $|P_e|$ versus the dimensionless distance from the surface, X , for different combinations of electrolyte valence. $a = 0.6$ nm, $(z_+ - z_-)c_b = 600$ mM, $T = 298$ K, $\epsilon = 6.94 \times 10^{-10}$ F/m, and $\sigma = 8.7 \times 10^{-2}$ C/m² were used as parameter values. (c) Variation of the critical total ion volume fraction in the bulk (χ_b), i.e., the electrolyte concentration at which Ψ reverses in sign, with dimensionless ion size (a/λ_B , where λ_B is Bjerrum length) for different combinations of cation and anion valence. (d) Plot of the critical bulk concentration $c_{b,\text{crit}}$, i.e., electrolyte concentration at which Ψ reverses sign with ion size.

has the smallest $\chi_{b,\text{crit}}$, indicating that multivalent electrolytes lead to EDL structure for smaller ion concentrations. In dimensional units, we find that the critical bulk concentration, $c_{b,\text{crit}}$, decreases sharply with an increase in the ion size a [Fig. 2(d)]. For $a \approx 1$ nm, the $c_{b,\text{crit}}$ can be as small as a few mM, indicating that the structure inside the EDL can start to appear even for dilute electrolyte concentrations. Consequently, at moderate and large concentrations, the ions can display a layered structure further away from the charged surface. This result is especially significant for ionic liquids where the ion sizes are large [22,24] and the ionic layers influence the effective Debye length [17,18]. Finally, the dependence of $\Psi(X)$ on surface charge density can also be crucial for ionic layering [57,64].

We compare the predictions of our proposed model with the steric PB model [22,24,26], the BSK model [26,31–33], a cDFT model based on the generalized van der Waals theory [38,39], and MC simulations based on the primitive-electrolyte model framework [45,46]. Since MC simulations do not rely on the continuum scale assumptions of the other approaches, we consider them to be the most accurate. Our results are summarized in Fig. 3.

The steric PB model predicts a monotonic $\Psi(X)$ for both 1:1 and 2:2 electrolytes and does not predict a sign

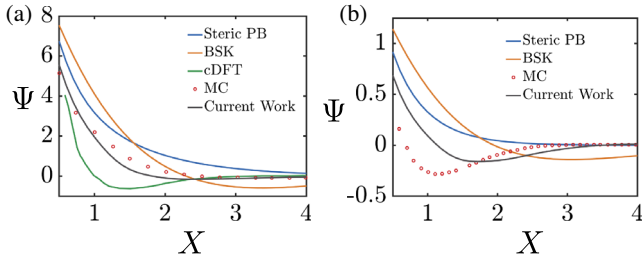


FIG. 3. Comparison of the proposed model with other models. Plot of the dimensionless electric potential Ψ versus the dimensionless distance from the surface X for the (a) 1:1 and (b) 2:2 electrolyte. The parameter values and the results for cDFT and MC simulations were extracted from Refs. [38] and [45,46]. The steric PB model was taken from Refs. [22,26], and the BSK model was adapted from Ref. [31].

reversal in potential (see Fig. 3). In contrast, the BSK model predicts a sign reversal in $\Psi(X)$ for both 1:1 and 2:2 electrolytes, unlike the MC simulation that only predicts the sign reversal for the 2:2 electrolyte. The cDFT yields a reversal in $\Psi(X)$, but the value of $\Psi(X)$ is significantly lower than the MC predictions. Finally, our proposed model yields $\Psi(X)$ closest to the MC predictions. More importantly, the proposed model shows a sign reversal in $\Psi(X)$ for 2:2 electrolytes, similar to the MC predictions. We observe qualitatively similar trends between the aforementioned models when compared to IET (see Fig. S3 in [57]) and molecular dynamics (see Fig. S4 in [57]). The quantitative disagreement between the proposed model and more computationally intensive models arise because we assume that ions act as point charges for distances greater than the closest approach and ignore the hard-sphere correlations in that region.

Since we treat ions as hard spheres below the distance of closest approach, our model is similar to the cDFT and the IET approaches. Yet, we are able to preserve the simplicity and computational appeal of the PB framework by excluding interactions that are less consequential and by using the lattice gas model to describe entropy. The intent of the BSK model is similar to our approach. However, it is unable to self-consistently capture the effect of ion size and electrolyte valence on charge oscillations because it relies on the correlation length scale to capture ion-ion correlations and overlooks the inherent nonlocal nature of these correlations. Nevertheless, our model is computationally more expensive than the BSK model and thus there is a trade-off between accuracy and computational ease (see Table S1 in [57] for a comparative analysis of different modeling approaches).

Next, we apply our model to an out-of-equilibrium phenomenon. We investigate the EDL charging process between flat plates (see Ref. [57] for details), typically studied using the PB models [23,62]. We consider the scenario where a binary electrolyte of concentration c_b , ion valences z_{\pm} , ion size a , and ion diffusivities D (assumed to

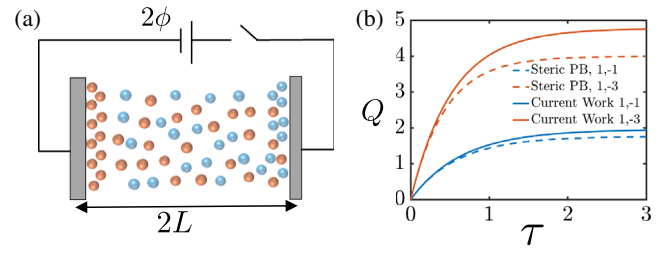


FIG. 4. Charging dynamics of electrical double layers in a planar geometry. (a) Schematic of the problem setup. (b) Plot of the absolute dimensionless charge stored inside EDLs, i.e., $Q = |\sigma|/[(|z|_+ + |z|_-)ec_0\lambda]$, with dimensionless time, i.e., $\tau = tD/(\lambda L)$. $\phi = 37.5$ mV, $a = 0.6$ nm, $(|z|_+ + |z|_-)c_b = 1$ M, $T = 298$ K, and $\epsilon = 6.94 \times 10^{-10}$ F/m. The dependence on L is absorbed in the definition of τ .

be equal), is brought in contact with two electrodes separated by a distance $2L$ [see Fig. 4(a)]. We assume that ion fluxes are zero across the electrodes and that $\lambda/L \ll 1$, where $\lambda = \sqrt{\epsilon k_B T / (\sum z_i^2 e^2 c_{bi})}$ is the Debye length. At $t = 0$, a potential difference of 2ϕ is applied such that EDLs develop at the electrodes. For $t > 0$, the potential drop and charge stored inside the EDLs increase with time. At steady state, the combined potential drop across the two EDLs equals 2ϕ and the total charge saturates. We plot the magnitude of dimensionless charge stored inside the EDL, i.e., $Q = |\sigma|/[(|z|_+ + |z|_-)ec_b\lambda]$, with dimensionless time, i.e., $\tau = tD/(\lambda L)$ in Fig. 4(b). Our model yields a larger Q than the steric PB model for both 1:1 and 1:3 electrolytes. In fact, the increase is larger for the 1:3 electrolyte because of a higher tendency for EDL structuring, which in turn increases the effective Debye length that ultimately increases the capacity to store charge. Finally, an increase in effective Debye length also increases the timescale of charging [62]. In summary, since our model is based on the PB framework, it is able to reveal the subtle features of a nonequilibrium phenomenon that may be otherwise overlooked.

Looking forward, our model can be extended to two-dimensional and three-dimensional EDLs that will yield insights into the arrangement of ions tangential to the surface. In addition, our methodology can be employed to probe the effect of shape anisotropy on the screening potential, which will be especially useful for large and shape-asymmetric ions. Furthermore, our approach can be extended to derive modified Nernst–Planck equations to analyze electrophoresis [58], diffusiophoresis [59,61], charging of supercapacitors [62,63], desalination [5,6], and soil-based phenomena [11,12]. Our model can also be exploited to obtain relationships for colloidal stability, such as in the Derjaguin–Landau–Verwey–Overbeek theory. The oscillations in ion concentration profiles will also be crucial for understanding the structure of ionic liquids. Lastly, we highlight that, since our approach

already includes the effect of ion size, it can be adapted for concentrated electrolytes, large potentials, and mixtures of electrolytes [65].

We thank the Andlinger Center for Energy and the Environment at Princeton University, the National Science Foundation (CBET—1702693), and the Air Force Office of Scientific Research (AFOSR Grant No. FA9550-14-1-0254) for financial support.

*ankur.gupta@colorado.edu

†hastone@princeton.edu

- [1] P. Simon and Y. Gogotsi, Materials for electrochemical capacitors, *Nat. Mater.* **7**, 845 (2008).
- [2] B. Conway and W. Pell, Double-layer and pseudocapacitance types of electrochemical capacitors and their applications to the development of hybrid devices, *J. Solid State Electrochem.* **7**, 637 (2003).
- [3] H. Wang and L. Pilon, Physical interpretation of cyclic voltammetry for measuring electric double layer capacitances, *Electrochim. Acta* **64**, 130 (2012).
- [4] A. G. Rajan, J. M. P. Martinez, and E. A. Carter, Why do we use the materials and operating conditions we use for heterogeneous (photo) electrochemical water splitting?, *ACS Catal.* **10**, 11177 (2020).
- [5] P. M. Biesheuvel and M. Z. Bazant, Nonlinear dynamics of capacitive charging and desalination by porous electrodes, *Phys. Rev. E* **81**, 031502 (2010).
- [6] K. T. Chu and M. Z. Bazant, Nonlinear electrochemical relaxation around conductors, *Phys. Rev. E* **74**, 011501 (2006).
- [7] J. Palacci, S. Sacanna, A. P. Steinberg, D. J. Pine, and P. M. Chaikin, Living crystals of light-activated colloidal surfers, *Science* **339**, 936 (2013).
- [8] A. Banerjee, I. Williams, R. N. Azevedo, M. E. Helgeson, and T. M. Squires, Solute-inertial phenomena: Designing long-range, long-lasting, surface-specific interactions in suspensions, *Proc. Natl. Acad. Sci. U.S.A.* **113**, 8612 (2016).
- [9] A. Aubret, M. Youssef, S. Sacanna, and J. Palacci, Targeted assembly and synchronization of self-spinning microgears, *Nat. Phys.* **14**, 1114 (2018).
- [10] S. Shin, E. Um, B. Sabass, J. T. Ault, M. Rahimi, P. B. Warren, and H. A. Stone, Size-dependent control of colloid transport via solute gradients in dead-end channels, *Proc. Natl. Acad. Sci. U.S.A.* **113**, 257 (2016).
- [11] A. P. Shapiro and R. F. Probstein, Removal of contaminants from saturated clay by electroosmosis, *Environ. Sci. Technol.* **27**, 283 (1993).
- [12] M. Cheng, G. Zeng, D. Huang, C. Yang, C. Lai, C. Zhang, and Y. Liu, Advantages and challenges of Tween 80 surfactant-enhanced technologies for the remediation of soils contaminated with hydrophobic organic compounds, *Chem. Eng. J.* **314**, 98 (2017).
- [13] D. F. Evans and H. Wennerstrom, *Colloidal Domain* (Wiley-Vch, New York, 1999).
- [14] J. Lyklema, *Fundamentals of Interface and Colloid Science* (Academic Press, London, 1995), Vol. 2.
- [15] S. Pennathur and J. G. Santiago, Electrokinetic transport in nanochannels. 1. Theory, *Anal. Chem.* **77**, 6772 (2005).
- [16] W. Sparreboom, A. van den Berg, and J. C. Eijkel, Principles and applications of nanofluidic transport, *Nat. Nanotechnol.* **4**, 713 (2009).
- [17] N. Gavish, D. Elad, and A. Yochelis, From solvent-free to dilute electrolytes: Essential components for a continuum theory, *J. Phys. Chem. Lett.* **9**, 36 (2018).
- [18] M. A. Gebbie, M. Valtiner, X. Banquy, E. T. Fox, W. A. Henderson, and J. N. Israelachvili, Ionic liquids behave as dilute electrolyte solutions, *Proc. Natl. Acad. Sci. U.S.A.* **110**, 9674 (2013).
- [19] Y. Avni, R. M. Adar, and D. Andelman, Charge oscillations in ionic liquids: A microscopic cluster model, *Phys. Rev. E* **101**, 010601(R) (2020).
- [20] A. A. Lee, C. S. Pérez-Martínez, A. M. Smith, and S. Perkin, Scaling Analysis of the Screening Length in Concentrated Electrolytes, *Phys. Rev. Lett.* **119**, 026002 (2017).
- [21] H. Wennerström, E. V. Estrada, J. Danielsson, and M. Oliveberg, Colloidal stability of the living cell, *Proc. Natl. Acad. Sci. U.S.A.* **117**, 10113 (2020).
- [22] M. S. Kilic, M. Z. Bazant, and A. Ajdari, Steric effects in the dynamics of electrolytes at large applied voltages. I. Double-layer charging, *Phys. Rev. E* **75**, 021502 (2007).
- [23] M. S. Kilic, M. Z. Bazant, and A. Ajdari, Steric effects in the dynamics of electrolytes at large applied voltages. II. Modified Poisson-Nernst-Planck equations, *Phys. Rev. E* **75**, 021503 (2007).
- [24] A. A. Kornyshev, Double-layer in ionic liquids: Paradigm change?, *J. Phys. Chem. B* **111**, 5545 (2007).
- [25] I. Borukhov, D. Andelman, and H. Orland, Adsorption of large ions from an electrolyte solution: A modified Poisson-Boltzmann equation, *Electrochim. Acta* **46**, 221 (2000).
- [26] A. Gupta and H. A. Stone, Electrical double layers: Effects of asymmetry in electrolyte valence on steric effects, dielectric decrement, and ion-ion correlations, *Langmuir* **34**, 11971 (2018).
- [27] D. Ben-Yaakov, D. Andelman, D. Harries, and R. Podgornik, Beyond standard Poisson-Boltzmann theory: Ion-specific interactions in aqueous solutions, *J. Phys. Condens. Matter* **21**, 424106 (2009).
- [28] Y. Nakayama and D. Andelman, Differential capacitance of the electric double layer: The interplay between ion finite size and dielectric decrement, *J. Chem. Phys.* **142**, 044706 (2015).
- [29] M. M. Hatlo, R. Van Roij, and L. Lue, The electric double layer at high surface potentials: The influence of excess ion polarizability, *Europhys. Lett.* **97**, 28010 (2012).
- [30] M. M. Hatlo and L. Lue, Electrostatic interactions of charged bodies from the weak-to the strong-coupling regime, *Europhys. Lett.* **89**, 25002 (2010).
- [31] M. Z. Bazant, B. D. Storey, and A. A. Kornyshev, Double Layer in Ionic Liquids: Overscreening Versus Crowding, *Phys. Rev. Lett.* **106**, 046102 (2011).
- [32] B. D. Storey and M. Z. Bazant, Effects of electrostatic correlations on electrokinetic phenomena, *Phys. Rev. E* **86**, 056303 (2012).
- [33] C. D. Santangelo, Computing counterion densities at intermediate coupling, *Phys. Rev. E* **73**, 041512 (2006).

- [34] R. F. Stout and A. S. Khair, A continuum approach to predicting electrophoretic mobility reversals, *J. Fluid Mech.* **752**, R1 (2014).
- [35] Z. Li and J. Wu, Density-functional theory for the structures and thermodynamic properties of highly asymmetric electrolyte and neutral component mixtures, *Phys. Rev. E* **70**, 031109 (2004).
- [36] D. Henderson, S. Lamperski, Z. Jin, and J. Wu, Density functional study of the electric double layer formed by a high density electrolyte, *J. Phys. Chem. B* **115**, 12911 (2011).
- [37] J. Wu, T. Jiang, D.-e. Jiang, Z. Jin, and D. Henderson, A classical density functional theory for interfacial layering of ionic liquids, *Soft Matter* **7**, 11222 (2011).
- [38] E. Boyle, L. Scriven, and H. Davis, The generalized van der Waals theory applied to the electrical double layer, *J. Chem. Phys.* **86**, 2309 (1987).
- [39] Z. Tang, L. Mier-y-Teran, H. Davis, L. Scriven, and H. White, Non-local free-energy density-functional theory applied to the electrical double layer: Part I: Symmetrical electrolytes, *Mol. Phys.* **71**, 369 (1990).
- [40] R. H. Nilson and S. K. Griffiths, Influence of atomistic physics on electro-osmotic flow: An analysis based on density functional theory, *J. Chem. Phys.* **125**, 164510 (2006).
- [41] J. W. Lee, R. H. Nilson, J. A. Templeton, S. K. Griffiths, A. Kung, and B. M. Wong, Comparison of molecular dynamics with classical density functional and Poisson–Boltzmann theories of the electric double layer in nanochannels, *J. Chem. Theory Comput.* **8**, 2012 (2012).
- [42] C. N. Patra and S. K. Ghosh, Structure of electric double layers: A self-consistent weighted-density-functional approach, *J. Chem. Phys.* **117**, 8938 (2002).
- [43] F. Jiménez-Ángeles and M. Lozada-Cassou, On the regimes of charge reversal, *J. Chem. Phys.* **128**, 174701 (2008).
- [44] F. Jiménez-Ángeles, G. Odriozola, and M. Lozada-Cassou, Electrolyte distribution around two like-charged rods: Their effective attractive interaction and angular dependent charge reversal, *J. Chem. Phys.* **124**, 134902 (2006).
- [45] G. Torrie and J. Valleau, Electrical double layers. I. Monte Carlo study of a uniformly charged surface, *J. Chem. Phys.* **73**, 5807 (1980).
- [46] G. Torrie and J. Valleau, Electrical double layers. 4. Limitations of the Gouy–Chapman theory, *J. Chem. Phys.* **86**, 3251 (1982).
- [47] D. Henderson and D. Boda, Insights from theory and simulation on the electrical double layer, *Phys. Chem. Chem. Phys.* **11**, 3822 (2009).
- [48] D. Boda, W. R. Fawcett, D. Henderson, and S. Sokolowski, Monte Carlo, density functional theory, and Poisson–Boltzmann theory study of the structure of an electrolyte near an electrode, *J. Chem. Phys.* **116**, 7170 (2002).
- [49] A. Martín-Molina, J. A. Maroto-Centeno, R. Hidalgo-Alvarez, and M. Quesada-Pérez, Charge reversal in real colloids: Experiments, theory and simulations, *Colloids Surf. A* **319**, 103 (2008).
- [50] P. S. Crozier, R. L. Rowley, and D. Henderson, Molecular-dynamics simulations of ion size effects on the fluid structure of aqueous electrolyte systems between charged model electrodes, *J. Chem. Phys.* **114**, 7513 (2001).
- [51] R. Messina, E. González-Tovar, M. Lozada-Cassou, and C. Holm, Overcharging: The crucial role of excluded volume, *Europhys. Lett.* **60**, 383 (2002).
- [52] M. Deserno, F. Jiménez-Ángeles, C. Holm, and M. Lozada-Cassou, Overcharging of DNA in the presence of salt: Theory and simulation, *J. Phys. Chem. B* **105**, 10983 (2001).
- [53] A. Kubíčková, T. Křížek, P. Coufal, M. Vazdar, E. Wernersson, J. Heyda, and P. Jungwirth, Overcharging in Biological Systems: Reversal of Electrophoretic Mobility of Aqueous Polyaspartate by Multivalent Cations, *Phys. Rev. Lett.* **108**, 186101 (2012).
- [54] L. Joly, C. Ybert, E. Trizac, and L. Bocquet, Hydrodynamics within the Electric Double Layer on Slipping Surfaces, *Phys. Rev. Lett.* **93**, 257805 (2004).
- [55] E. Waisman and J. L. Lebowitz, Mean spherical model integral equation for charged hard spheres I. Method of solution, *J. Chem. Phys.* **56**, 3086 (1972).
- [56] E. Waisman and J. L. Lebowitz, Mean spherical model integral equation for charged hard spheres II. Results, *J. Chem. Phys.* **56**, 3093 (1972).
- [57] See Supplemental Material at <http://link.aps.org/supplemental/10.1103/PhysRevLett.125.188004> for the detailed description of experimental, theoretical, and numerical methods.
- [58] R. W. O’Brien and L. R. White, Electrophoretic mobility of a spherical colloidal particle, *J. Chem. Soc., Faraday Trans. 2* **74**, 1607 (1978).
- [59] A. Gupta, B. Rallabandi, and H. A. Stone, Diffusiophoretic and diffusioosmotic velocities for mixtures of valence-asymmetric electrolytes, *Phys. Rev. Fluids* **4**, 043702 (2019).
- [60] D. Velegol, A. Garg, R. Guha, A. Kar, and M. Kumar, Origins of concentration gradients for diffusiophoresis, *Soft Matter* **12**, 4686 (2016).
- [61] A. Gupta, S. Shim, and H. A. Stone, Diffusiophoresis: From dilute to concentrated electrolytes, *Soft Matter* **16**, 6975 (2020).
- [62] M. Z. Bazant, K. Thornton, and A. Ajdari, Diffuse-charge dynamics in electrochemical systems, *Phys. Rev. E* **70**, 021506 (2004).
- [63] A. Gupta, P. J. Zuk, and H. A. Stone, Charging Dynamics of Overlapping Double Layers in a Cylindrical Nanopore, *Phys. Rev. Lett.* **125**, 076001 (2020).
- [64] J. P. de Souza, Z. A. H. Goodwin, M. McEldrew, A. A. Kornyshev, and M. Z. Bazant, Interfacial Layering in the Electrical Double Layer of Ionic Liquids, *Phys. Rev. Lett.* **125**, 116001 (2020).
- [65] A. Gupta, S. Shim, L. Issah, C. McKenzie, and H. A. Stone, Diffusion of multiple electrolytes cannot be treated independently: Model predictions with experimental validation, *Soft Matter* **15**, 9965 (2019).